Uludağ Üniversitesi Tıp Fakültesi Dergisi
Journal of Uludağ University Medical Faculty
52, 1966222, 2026
DOI: https://doi.org/10.32708/uutfd.1966222

ORIGINAL RESEARCH

Preliminary Evaluation of Interocular Agreement and Biometric Associations of Cone Photoreceptor Metrics in Healthy Young Adults Using Confocal Retinal Imaging

Serap KARACA[1], Osman KIZILAY[2], Furkan KIRIK[3], Bilge BATU OTO[4], Gökhan ÇELİK[2]

[1] Göztepe Prof. Dr. Süleyman Yalçın City Hospital, Department of Ophthalmology, İstanbul, Türkiye.
[2] Zeynep Kamil Maternity and Children's Disease Training and Research Hospital, Department of Ophthalmology, İstanbul, Türkiye.
[3] Bezmialem Vakıf University Faculty of Medicine Hospital, Department of Ophthalmology, İstanbul, Türkiye.
[4] İstanbul University, Cerrahpaşa Medical Faculty Hospital, Department of Ophthalmology, İstanbul, Türkiye.

ABSTRACT

This study evaluated the interocular agreement and within-eye repeatability of cone photoreceptor metrics measured using a confocal cone analysis system in healthy young adults, as well as their associations with ocular dominance and axial length. This cross-sectional study included 94 eyes from 47 healthy participants. Cone density and cone diameter were measured from fovea-centered 3 × 3 mm images obtained using the MicroClear CRO system (MicroClear Biomedical Co., Ltd., Suzhou, China). Magnification-corrected and original uncorrected cone measurements were analyzed. Interocular agreement was assessed using paired comparisons, intraclass correlation coefficients (ICC), and Bland–Altman analysis. Within-eye repeatability was evaluated from two repeated measurements per eye using the within-subject standard deviation, coefficient of repeatability (CoR), ICC, and Bland–Altman analysis. Associations with axial length were examined using Spearman correlation and generalized estimating equation (GEE) models. No significant interocular differences were observed for magnification-corrected cone density (mean difference, −763 cells/mm²; 95% confidence interval [CI], −2,799 to 1,273; p = 0.455; ICC = 0.679) or cone diameter (mean difference, 0.07 µm; 95% CI, −0.12 to 0.27; p = 0.455; ICC = 0.359). After exclusion of four measurements with automated segmentation failure, within-eye repeatability was good for both cone density (CoR = 4,937 cells/mm²; ICC = 0.924) and cone diameter (CoR = 0.40 µm; ICC = 0.941). Cone photoreceptor parameters were also similar between dominant and nondominant eyes. At the participant level, magnification-corrected cone density showed a moderate negative correlation with axial length (Spearman ρ = −0.545; p < 0.001), and this association remained significant in the adjusted GEE model (β = −5,914.39 cells/mm²/mm; 95% CI, −8,567.73 to −3,261.06; p < 0.001). In contrast, axial length was not significantly associated with uncorrected cone density in either the participant-level correlation analysis (Spearman ρ = −0.121; p = 0.419) or the adjusted GEE model (β = −1,798.92 cells/mm²/mm; 95% CI, −4,104.46 to 506.62; p = 0.126). These findings indicate good within-eye repeatability after exclusion of segmentation-failure measurements, while the association between axial length and cone density was sensitive to the magnification-correction procedure and should therefore be interpreted cautiously.

Keywords: Cone photoreceptors. Confocal retinal imaging. Axial length. Interocular agreement. Ocular dominance. Cone density.

Konfokal Retinal Görüntüleme Kullanılarak Sağlıklı Genç Erişkinlerde Koni Fotoreseptör Parametrelerinin Gözler Arası Uyumunun ve Biyometrik İlişkilerinin Ön Değerlendirmesi

ÖZET

Bu çalışmada, sağlıklı genç erişkinlerde konfokal koni analiz sistemi kullanılarak ölçülen koni fotoreseptör parametrelerinin gözler arası uyumu ve göz içi tekrarlanabilirliği ile bu parametrelerin oküler dominans ve aksiyel uzunluk ile ilişkileri değerlendirildi. Bu kesitsel çalışmaya 47 sağlıklı katılımcının 94 gözü dahil edildi. Koni yoğunluğu ve koni çapı, MicroClear CRO sistemi (MicroClear Biomedical Co., Ltd., Suzhou, Çin) kullanılarak elde edilen fovea merkezli 3 × 3 mm görüntülerden ölçüldü. Magnifikasyon düzeltmesi uygulanmış ve orijinal düzeltilmemiş koni ölçümleri analiz edildi. Gözler arası uyum, eşleştirilmiş karşılaştırmalar, sınıf içi korelasyon katsayıları (ICC) ve Bland–Altman analizi kullanılarak değerlendirildi. Göz içi tekrarlanabilirlik, her gözden elde edilen iki tekrarlı ölçüm kullanılarak denek içi standart sapma, tekrarlanabilirlik katsayısı (CoR), ICC ve Bland–Altman analizi ile değerlendirildi. Aksiyel uzunluk ile ilişkiler Spearman korelasyon analizi ve genelleştirilmiş tahmin denklemi (GEE) modelleri kullanılarak incelendi. Magnifikasyon düzeltmesi uygulanmış koni yoğunluğu (ortalama fark, −763 hücre/mm²; %95 güven aralığı [GA], −2.799 ile 1.273; p = 0,455; ICC = 0,679) veya koni çapı (ortalama fark, 0,07 µm; %95 GA, −0,12 ile 0,27; p = 0,455; ICC = 0,359) açısından gözler arasında anlamlı fark saptanmadı. Otomatik segmentasyon hatası bulunan dört ölçüm dışlandıktan sonra, hem koni yoğunluğu (CoR = 4.937 hücre/mm²; ICC = 0,924) hem de koni çapı (CoR = 0,40 µm; ICC = 0,941) için göz içi tekrarlanabilirlik yüksekti. Koni fotoreseptör parametreleri dominant ve nondominant gözler arasında da benzerdi. Katılımcı düzeyinde, magnifikasyon düzeltmesi uygulanmış koni yoğunluğu ile aksiyel uzunluk arasında orta düzeyde negatif korelasyon saptandı (Spearman ρ = −0,545; p < 0,001) ve bu ilişki düzeltilmiş GEE modelinde de anlamlılığını korudu (β = −5.914,39

hücre/mm²/mm; %95 GA, −8.567,73 ile −3.261,06; p < 0,001). Buna karşılık, aksiyel uzunluk ile düzeltilmemiş koni yoğunluğu arasında katılımcı düzeyindeki korelasyon analizinde (Spearman ρ = −0,121; p = 0,419) veya düzeltilmiş GEE modelinde (β = −1.798,92 hücre/mm²/mm; %95 GA, −4.104,46 ile 506,62; p = 0,126) anlamlı ilişki saptanmadı. Bu bulgular, segmentasyon hatası bulunan ölçümler dışlandığında göz içi tekrarlanabilirliğin iyi olduğunu, aksiyel uzunluk ile koni yoğunluğu arasındaki ilişkinin ise magnifikasyon düzeltme işlemine duyarlı olduğunu ve bu nedenle dikkatle yorumlanması gerektiğini göstermektedir.

Anahtar Kelimeler: Koni fotoreseptörleri. Konfokal retinal görüntüleme. Aksiyel uzunluk. Gözler arası uyum. Oküler dominans. Koni yoğunluğu.

Date Received: 8.June.2026
Date Accepted: 12.September.2026

Dr. Serap KARACA
Göztepe Prof. Dr. Süleyman Yalçın City Hospital,
Department of Ophthalmology, İstanbul, Türkiye.
E-mail: dr.serap44@gmail.com

AUTHORS' ORCID INFORMATION
Serap KARACA: 0000-0003-0325-2804
Osman KIZILAY: 0000-0002-0948-3550
Furkan KIRIK: 0000-0001-5846-8536
Bilge BATU OTO: 0000-0002-9729-2577
Gökhan ÇELIK: 0000-0003-2111-0420

Vision depends on light being transmitted through the ocular media and focused onto the retina, particularly the fovea. Retinal photoreceptors are responsible for detecting light stimuli and converting them into neural signals transmitted to the visual cortex[1]. Although cones account for only about 5% of all retinal photoreceptors, they play a role in color perception, contrast sensitivity, and high-resolution vision[2]. Cone photoreceptor density is considered a key indicator of foveal structure and function and is widely used to assess the effects of visual development, aging, refractive status, and retinal diseases on the photoreceptor mosaic[3]. Previous studies have demonstrated that cone density and spatial distribution may be influenced by various factors, including age, axial length (AL), refractive errors, and retinal stretching associated with eye growth[4-8].

Accurate visualization of cone photoreceptors is important for understanding normal retinal structure and detecting microstructural changes associated with retinal disorders [9]. Adaptive optics (AO) and adaptive optics scanning laser ophthalmoscopy (AOSLO) have become established techniques for in vivo imaging of the cone mosaic [10, 11]. By compensating for optical aberrations within the ocular media, these systems provide high-resolution, noninvasive visualization of individual photoreceptors. However, their routine clinical application remains limited because of high cost, technical complexity, prolonged image acquisition and processing times, and the requirement for specialized expertise[11]. The MicroClear CRO system is a recently developed confocal retinal imaging system that automatically identifies cone photoreceptors within a 3 × 3 mm area centered on the fovea and provides quantitative measurements of cone density and cone diameter through image analysis. Although AO-based technologies are widely used to quantify cone photoreceptor mosaics, data on cone measurements obtained using automated confocal cone analysis platforms remain limited.

Clinical data on cone photoreceptor measurements obtained using the MicroClear CRO system in healthy human eyes remain limited. The potential value of this platform lies not in replacing conventional AO systems, but in providing a more accessible and automated approach for quantitative cone photoreceptor assessment. Therefore, the present study aimed to provide a preliminary clinical evaluation of cone photoreceptor metrics obtained using the MicroClear CRO system in healthy young adults. Specifically, within-eye repeatability and interocular agreement of cone photoreceptor measurements were evaluated, dominant and nondominant eyes were compared, and the associations of cone density with AL and spherical equivalent (SE) were investigated. The study also aimed to provide preliminary device-specific reference values for cone photoreceptor metrics obtained with this automated confocal imaging system in this population.

Materials and Methods

Patient Selection

This cross-sectional study included healthy young adult participants who were evaluated at the ophthalmology clinic of Zeynep Kamil Maternity and Children's Diseases Training and Research Hospital. The study protocol was approved by the ethics committee of the hospital (Ethics Committee Decision No: 97). The research was conducted in accordance with the principles of the Declaration of Helsinki, and written informed consent was obtained from all participants.

Participants were selected from among healthy volunteers. Inclusion criteria were age between 18 and 45 years, best-corrected visual acuity (BCVA) of 20/25 or better, intraocular pressure between 10 and 21 mm Hg, SE ranging from −3.00 to 0.00 diopters, astigmatism not exceeding 1.00 diopter, and absence of ocular or systemic disease. Exclusion criteria were previous ocular trauma or surgery, amblyopia, strabismus, hyperopia or high myopia, corneal opacity or other media opacity precluding high-quality imaging, any retinal or optic nerve pathology, systemic disease with potential ocular involvement, and inability to obtain an analyzable image because of

poor fixation or inadequate image quality. Both eyes of each eligible participant were included. The paired-eye structure of the dataset was considered in the statistical analysis to account for interocular correlation.

Ophthalmic Examination and Cone Photoreceptor Imaging

All participants underwent a comprehensive ophthalmic examination before imaging. BCVA was measured using a Snellen chart and converted to logarithm of the minimum angle of resolution (logMAR) values for analysis. Intraocular pressure was measured using Goldmann applanation tonometry. Objective refraction was obtained with an automated refractometer (Nidek HandyRef-K, Nidek Co., Ltd., Gamagori, Japan), and SE was calculated as the spherical power plus one-half of the cylindrical power. AL was measured using the Lenstar LS 900 optical biometer (Haag-Streit AG, Bern, Switzerland). Ocular dominance was determined using the hole-in-the-card test at a viewing distance of 3 m. All examinations and measurements were performed under standardized conditions by the same experienced ophthalmologist.

Cone photoreceptor imaging was performed after pupil dilation using the MicroClear CRO cone analysis system (MicroClear Biomedical Co., Ltd., Suzhou, China). The device acquires confocal fundus images using a 785-nm laser and analyzes cone photoreceptor morphology within a 3 × 3-mm area centered on the fovea using dedicated cone recognition and analysis software. Imaging was performed in a dimly illuminated room using the device's internal fixation target. For each eye, at least two images were acquired. Images were considered unsuitable for analysis when image quality was below 80%, fixation was unstable, or the automated analysis did not generate valid quantitative cone measurements. In such cases, imaging was repeated until an analyzable image was obtained. When more than one analyzable image was available, the image with the highest quality and most stable fixation was selected for the primary cross-sectional analyses. Two repeated measurements obtained during the same imaging session from each eye were used to assess within-eye repeatability. Representative cone photoreceptor images obtained with the MicroClear CRO system are shown in Figure 1.

The device software automatically defined a 3 × 3 mm analysis area centered on the fovea. Cone photoreceptors within this area were automatically identified and segmented using the proprietary cone recognition and analysis software. Vascular structures were not displayed as cone photoreceptors in the automated cone analysis output, and no additional manual vessel masking or correction was performed by the investigators. Cone density was defined as the number of detected cones per square millimeter (cells/mm²), and the reported cone density represented the global mean across the entire 3 × 3 mm analysis area. Mean cone diameter, expressed as μm, was also automatically generated by the device software using its proprietary cone recognition and analysis algorithm, without manual measurement or modification by the investigators. The exact calculation used to derive mean cone diameter is not disclosed by the manufacturer.

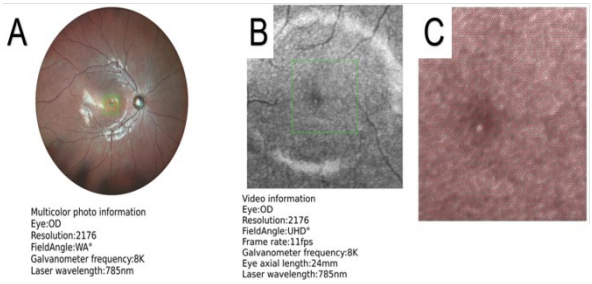

Figure 1:
Representative images obtained using the MicroClear CRO cone analysis system. (A) Multicolor fundus image showing the foveal reference area; (B) infrared confocal image showing the 3 × 3 mm fovea-centered analysis area; and (C) automated cone mosaic map showing identified and segmented cone photoreceptors used for the calculation of cone density and mean cone diameter.

To account for ocular magnification, the measured AL of each eye was entered into the device software, which automatically applied an AL-based magnification correction to the cone measurements. The device uses a default AL setting of 24.00 mm, and measurements obtained with this default setting were retained as the uncorrected values. After the measured AL of each eye was entered, the corresponding magnification-corrected cone density and cone diameter values generated by the software were recorded. The magnification correction is based on the Littmann–Bennett principle and refined according to the optical characteristics of the MicroClear system. The magnification factor used by the system was calculated as 0.0492 × AL − 0.1818, where AL represents axial length in millimeters. Keratometric parameters were not included in the magnification correction. Both uncorrected and magnification-corrected measurements were retained for subsequent analyses. Magnification-corrected values were used in the primary analyses, whereas uncorrected values were additionally analyzed to assess the potential influence of AL-based magnification correction on the observed association between AL and cone density.

Statistical Analysis

Statistical analyses were performed using Stata version 19.0 (StataCorp LLC, College Station, TX,

USA). Continuous variables were summarized as mean ± standard deviation or median (interquartile range), as appropriate, and categorical variables as frequency and percentage. Normality was assessed using the Shapiro-Wilk test and visual inspection of histograms and quantile-quantile plots.

The primary analysis evaluated interocular differences and agreement in magnification-corrected cone density and cone diameter between right and left eyes. Paired comparisons were performed using paired-samples t tests or Wilcoxon signed-rank tests, as appropriate. Interocular agreement was assessed using intraclass correlation coefficients (ICCs) based on a two-way mixed-effects model for absolute agreement, together with Bland-Altman analysis. Secondary analyses compared ocular and cone photoreceptor parameters between dominant and nondominant eyes. Associations of cone density with age, SE, AL, and cone diameter were evaluated at the participant level to avoid nonindependence between fellow eyes. For eye-specific variables, the mean of the right and left eyes was calculated for each participant, and Spearman rank correlations were performed using the resulting 47 independent participant-level observations. Analyses were performed separately using magnification-corrected and uncorrected measurements.

Within-eye repeatability was assessed using two repeated magnification-corrected measurements per eye for cone density and cone diameter. Repeatability was quantified using the within-subject standard deviation (wsSD), coefficient of repeatability (CoR; $1.96 \times \sqrt{2} \times$ wsSD), within-subject coefficient of variation (CV), and ICC based on a two-way random-effects model for absolute agreement of single measurements [ICC (2,1)]. Agreement between repeated measurements was also assessed using Bland-Altman analysis. One repeat measurement in each of four eyes showed automated segmentation failure. These measurements were identified by visual inspection of the segmentation output, which showed erroneous cone detection in areas without discernible photoreceptors. Markedly implausible quantitative values were also observed. Segmentation failure occurred in 4 of 188 repeated measurements (2.1%). Repeatability analyses were therefore performed both with and without these measurements, with the segmentation-failure measurements excluded from the primary analysis.

Because both eyes from each participant were included, generalized estimating equation (GEE) models with an exchangeable working correlation structure and robust standard errors were used to account for within-participant correlation between fellow eyes. GEE was selected to estimate population-averaged associations while accounting for the correlated paired-eye data, rather than participant-specific effects. Cone density was modeled as the dependent variable, with AL as the primary independent variable. Adjusted models additionally included age, sex, and SE. The association between sex and magnification-corrected cone diameter was also evaluated using a GEE model adjusted for age, AL, and SE. Given the biological relationship between AL and SE, potential collinearity between these variables was considered when interpreting the adjusted models. Sensitivity analyses were performed after exclusion of cone density outliers identified using the 1.5 × interquartile range rule. Because AL was incorporated into the magnification correction of cone density, analyses examining the association between AL and magnification-corrected cone density were considered exploratory. Given the exploratory nature of the study, no formal adjustment for multiple comparisons was applied; therefore, secondary and exploratory findings were interpreted cautiously. All tests were two-sided, and $P < 0.05$ was considered statistically significant.

Results

Participant and Ocular Characteristics

The study included 94 eyes of 47 healthy participants, including 19 men (40.4%) and 28 women (59.6%). The mean age was 30.0 ± 5.0 years. The median SE was −0.75 diopters (IQR, −1.25 to −0.25), and the mean AL was 23.57 ± 0.93 mm. The mean magnification-corrected cone diameter was 5.91 ± 0.59 μm, and the median magnification-corrected cone density was 42,945 cells/mm² (IQR, 38,597–49,525). During image acquisition, four initial images were considered unsuitable for analysis and were therefore reacquired. These were separate from the repeat measurements excluded because of automated segmentation failure. Ultimately, analyzable images were obtained for all 94 eyes, and no eye was excluded from the final analysis because of unsuccessful imaging. The demographic, biometric, and cone photoreceptor parameters are summarized in Table I.

Interocular Differences and Agreement

No systematic interocular difference was observed in magnification-corrected cone density between right and left eyes. The mean right-left difference was −763 cells/mm² (95% CI, −2,799 to 1,273; P = 0.455). The interocular correlation for magnification-corrected cone density was moderate (r = 0.677), and the ICC was 0.679. Bland-Altman analysis showed a mean bias of −763 cells/mm², with 95% limits of agreement ranging from −14,353 to 12,828 cells/mm², indicating measurable interocular variability despite the absence of systematic bias.

Table I. Demographic, Ocular Biometric, and Cone Photoreceptor Characteristics of Healthy Young Adults

Variable	Value
Participant-Level Characteristics	
Participants, n	47
Age (years), mean ± SD	30.0 ± 5.0
Sex, male/female, n (%)	19 (40.4) / 28 (59.6)
Dominant eye, right/left, n (%)	22 (46.8) / 25 (53.2)
Eye-Level Characteristics	
Eyes, n	94
Right/left eyes, n (%)	47 (50.0) / 47 (50.0)
Spherical equivalent (D), median (IQR)	−0.75 (−1.25 to −0.25)
Axial length (mm), mean ± SD	23.57 ± 0.93
Magnification-corrected cone diameter (µm), mean ± SD	5.91 ± 0.59
Magnification-corrected cone density (cells/mm²), median (IQR)	42,945 (38,597 to 49,525)

Abbreviations: D, diopters; IQR, interquartile range; SD, standard deviation.
Cone metrics shown in the table are magnification-corrected values derived from the measurements obtained using the MicroClear CRO confocal cone analysis system.

No systematic right-left difference was observed in magnification-corrected cone diameter, with a mean difference of 0.07 µm (95% CI, −0.12 to 0.27; P = 0.455). The interocular correlation for magnification-corrected cone diameter was weaker (r = 0.357), with an ICC of 0.359. Thus, interocular agreement was moderate for cone density and poor for cone diameter, despite the absence of statistically significant systematic interocular differences. These findings are summarized in Table II.

Within-Eye Repeatability

After exclusion of four repeat measurements with automated segmentation failure, 90 eyes were included in the primary repeatability analysis. Repeatability was good for both cone diameter and cone density. For cone diameter, the wsSD was 0.15 µm, the CoR was 0.40 µm, and the ICC was 0.941 (95% CI, 0.910–0.960). For cone density, the corresponding values were 1,781 cells/mm², 4,937 cells/mm², and 0.924 (95% CI, 0.890–0.950), respectively. Bland–Altman analysis showed small mean differences between repeated measurements (+0.03 µm for cone diameter and +396 cells/mm² for cone density), with 95% limits of agreement of −0.37 to 0.43 µm and −4,507 to 5,298 cells/mm², respectively (Figure 2). When the four segmentation-failure measurements were retained, repeatability was substantially reduced (Supplementary Table SI).

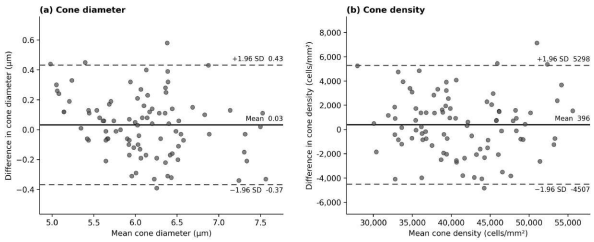

Figure 2:
Bland–Altman plots of within-eye repeatability for cone photoreceptor measurements. (A) Cone diameter and (B) cone density. The solid line represents the mean difference between repeated measurements, and the dashed lines represent the 95% limits of agreement. Analyses shown are based on the primary repeatability dataset after exclusion of four repeat measurements with automated segmentation failure.

Dominant Versus Nondominant Eye Comparisons

No significant differences were observed between dominant and nondominant eyes in refractive, biometric, or cone photoreceptor parameters. The dominant-nondominant difference in magnification-

Table II. Interocular Differences and Agreement of Magnification-Corrected Cone Metrics Between Right and Left Eyes

Parameter	Right Eye	Left Eye	Mean difference, Right − Left (95% CI)	P Value	Interocular correlation (r)	ICC	95% Limits of Agreement
Cone density, cells/mm², mean ± SD	44,225 ± 8,580	44,988 ± 8,668	−763 (−2,799 to 1,273)	0.455	0.677	0.679	−14,353 to 12,828
Cone diameter (µm), mean ± SD	5.94 ± 0.59	5.87 ± 0.58	0.07 (−0.12 to 0.27)	0.455	0.357	0.359	−1.23 to 1.38
Axial length (mm), mean ± SD	23.59 ± 0.94	23.56 ± 0.94	0.03 (−0.03 to 0.10)	0.305	0.973	0.973	−0.39 to 0.46
Spherical equivalent (D), mean ± SD	−0.87 ± 0.80	−0.79 ± 0.80	−0.09 (−0.21 to 0.04)	0.188	0.849	0.847	−0.94 to 0.77

Abbreviations: CI, confidence interval; D, diopters; ICC, intraclass correlation coefficient; SD, standard deviation.
Paired comparisons were performed using paired-samples t tests. ICC was calculated using a two-way mixed-effects model for absolute agreement.

corrected cone density was −285 cells/mm² (95% CI, −2,332 to 1,762; P = 0.767). Magnification-corrected cone diameter was also similar between dominant and nondominant eyes, with a mean difference of 0.00 µm (95% CI, −0.20 to 0.20; P = 0.841). No significant differences were found for AL (difference, −0.003 mm; 95% CI, −0.067 to 0.061; P = 0.927) or SE (difference, 0.05 diopters; 95% CI, −0.08 to 0.18; P = 0.542). These findings are summarized in Table III.

Supplementary Table SI. Within-eye repeatability of cone diameter and cone density measurements, with and without four repeat measurements with automated segmentation failure

Analysis	n	Mean	wsSD	CoR, value (%)	Within-subject CV (%)	ICC (95% CI)
Cone diameter (µm)						
Segmentation-failure measurements excluded (primary)	90	6.11	0.15	0.40 (6.6)	2.4	0.941 (0.910 to 0.960)
All measurements included (sensitivity)	94	6.32	2.70	7.47 (118.2)	42.7	0.036 (−0.170 to 0.240)
Cone density (cells/mm²)						
Segmentation-failure measurements excluded (primary)	90	41,221	1,781	4,937 (12.0)	4.3	0.924 (0.890 to 0.950)
All measurements included (sensitivity)	94	41,986	13,671	37,893 (90.3)	32.6	0.110 (−0.090 to 0.300)

CI, confidence interval; n, number of eyes.
Data are derived from two repeated measurements per eye. Four repeat measurements with automated segmentation failure were excluded from the primary analysis and retained in the sensitivity analysis. The within-subject standard deviation (wsSD) was calculated from the residual mean square of a one-way analysis of variance, and the coefficient of repeatability (CoR) as $1.96 \times \sqrt{2} \times$ wsSD. CoR (%) and within-subject coefficient of variation (CV) are expressed relative to the grand mean. The repeatability intraclass correlation coefficient (ICC) was estimated using a two-way random-effects model for absolute agreement of single measurements [ICC(2,1)].

Associations Between Cone Density and Ocular Parameters

At the participant level, magnification-corrected cone density was not significantly correlated with age (Spearman ρ = 0.039; P = 0.796) or SE (ρ = 0.188; P = 0.205), whereas it showed a moderate negative correlation with AL (ρ = −0.545; P < 0.001) and a strong negative correlation with magnification-corrected cone diameter (ρ = −0.742; P < 0.001). In contrast, uncorrected cone density was not significantly correlated with age (ρ = 0.124; P = 0.407), SE (ρ = 0.063; P = 0.673), or AL (ρ = −0.121; P = 0.419), while it remained negatively correlated with uncorrected cone diameter (ρ = −0.669; P < 0.001). These results are summarized in Table IV.

Table III. Dominant Versus Nondominant Eye Comparisons of Magnification-Corrected Cone Metrics and Ocular Biometric Parameters

Parameter	Dominant Eye	Nondominant Eye	Difference, Dominant − Nondominant (95% CI)	P Value
Spherical equivalent, D, median (IQR)	−0.50 (−1.25 to −0.25)	−0.75 (−1.25 to −0.25)	0.05 (−0.08 to 0.18)	0.542
Axial length, mm, mean ± SD	23.57 ± 0.92	23.58 ± 0.95	−0.003 (−0.067 to 0.061)	0.927
Cone diameter, µm, mean ± SD	5.91 ± 0.51	5.91 ± 0.66	0.00 (−0.20 to 0.20)	0.841
Cone density, cells/mm², median (IQR)	42,999 (38,482 to 49,766)	42,881 (39,338 to 49,086)	−285 (−2,332 to 1,762)	0.767

Abbreviations: CI, confidence interval; D, diopters; IQR, interquartile range; SD, standard deviation.
P values were derived from paired analyses. Differences were calculated as dominant eye minus nondominant eye using paired eye-level data and therefore may not correspond exactly to the arithmetic difference between the reported summary statistics.

Table IV. Participant-Level Associations of Magnification-Corrected and Uncorrected Cone Density With Demographic, Refractive, and Biometric Parameters

Parameter	Magnification-Corrected Cone Density, Spearman ρ	P Value	Uncorrected Cone Density, Spearman ρ	P Value
Age, years	0.039	0.796	0.124	0.407
Spherical equivalent, D	0.188	0.205	0.063	0.673
Axial length, mm	−0.545	< 0.001	−0.121	0.419
Cone diameter, µm	−0.742	< 0.001	−0.669	< 0.001

Abbreviation: D, diopters.
Analyses were performed at the participant level (n = 47). For eye-specific variables, the mean of the right and left eyes was calculated for each participant before Spearman correlation analysis, thereby avoiding nonindependence between fellow eyes. For the cone diameter analysis, magnification-corrected cone density was correlated with magnification-corrected cone diameter, whereas uncorrected cone density was correlated with uncorrected cone diameter.

GEE and Sensitivity Analyses

In the GEE model accounting for inter-eye correlation, longer AL was significantly associated with lower magnification-corrected cone density in the unadjusted model (β = −5,122.79 cells/mm² per mm; 95% CI,

−7,175.71 to −3,069.86; P < 0.001) and after adjustment for age, sex, and SE (β = −5,914.39 cells/mm² per mm; 95% CI, −8,567.73 to −3,261.06; P < 0.001). This association remained significant in the outlier-excluded adjusted analysis (β = −4,971.84 cells/mm² per mm; 95% CI, −7,194.47 to −2,749.21; P < 0.001). In contrast, AL was not significantly associated with uncorrected cone density in the unadjusted GEE model (β = −1,120.67 cells/mm² per mm; 95% CI, −2,928.34 to 687.00; P = 0.224), the adjusted model (β = −1,798.92 cells/mm² per mm; 95% CI, −4,104.46 to 506.62; P = 0.126), or the outlier-excluded adjusted model (β = −1,118.18 cells/mm² per mm; 95% CI, −3,233.92 to 997.55; P = 0.300) (Table V).

Table V. Generalized Estimating Equation Analyses of the Association Between Axial Length and Magnification-Corrected and Uncorrected Cone Density

Outcome and Model	β, cells/mm² per mm	95% CI	P Value
Magnification-corrected cone density			
Unadjusted GEE	−5,122.79	−7,175.71 to −3,069.86	< 0.001
Adjusted GEE	−5,914.39	−8,567.73 to −3,261.06	< 0.001
Adjusted GEE (outlier-excluded)	−4,971.84	−7,194.47 to −2,749.21	< 0.001
Uncorrected cone density			
Unadjusted GEE	−1,120.67	−2,928.34 to 687.00	0.224
Adjusted GEE	−1,798.92	−4,104.46 to 506.62	0.126
Adjusted GEE (outlier-excluded)	−1,118.18	−3,233.92 to 997.55	0.300

Abbreviations: CI, confidence interval; GEE, generalized estimating equations.
β coefficients represent the change in cone density (cells/mm²) per 1-mm increase in axial length. GEE models accounted for participant-level clustering using an exchangeable correlation structure and robust standard errors. Adjusted models included age, sex, and spherical equivalent. Outlier-excluded analyses excluded the participant with both eyes identified as magnification-corrected cone density outliers using the 1.5 × interquartile range criterion. Uncorrected cone density values represent measurements obtained before magnification correction.

Sex was not independently associated with magnification-corrected cone density (β = −1,443.72 cells/mm²; 95% CI, −5,615.98 to 2,728.54; P = 0.498) or cone diameter (β = 0.135 μm; 95% CI, −0.126 to 0.396; P = 0.310) after adjustment for age, AL, and SE.

Discussion and Conclusion

The present study provides a preliminary clinical evaluation of cone photoreceptor metrics obtained using the MicroClear CRO confocal cone analysis system in healthy young adults. Clinical data obtained with this platform in healthy human eyes remain limited. The main findings were good within-eye repeatability after exclusion of measurements with automated segmentation failure; the absence of systematic interocular differences in cone density and cone diameter, despite moderate interocular agreement for cone density and poor agreement for cone diameter; and the lack of ocular dominance-related differences in cone photoreceptor parameters. In addition, AL was inversely associated with magnification-corrected cone density, but this association was markedly attenuated and no longer statistically significant when uncorrected cone density was analyzed. The study also provides preliminary device-specific reference values for cone photoreceptor metrics obtained with this automated confocal imaging platform in this population.

In the literature, reported factors associated with cone density loss include AL, aging, and retinal diseases[14-16]. The inverse relationship between AL and cone density observed in our study is consistent with previous reports using AO, AOSLO, and confocal imaging[5, 17]. Tumahai et al.[6] reported in an AO study of 167 eyes from 101 subjects aged 6–78 years that greater AL was associated with lower cone density. Similarly, Park et al.[18] found a significant negative correlation between AL and cone density using AOSLO in 192 eyes of 192 individuals, while Zhou et al.[4] reported reduced linear cone density at both 3° and 5° eccentricities and decreased cone regularity with increasing AL. Liang et al.[7] also found an inverse association between cone density and AL in multivariable analysis, and Legras et al. [19] demonstrated decreasing cone density with AL elongation using the Rtx1 adaptive optics camera, attributing this finding to retinal stretching. Because cone density in the present study represents a global mean across the entire 3 × 3 mm fovea-centered analysis area, direct numerical comparisons with AO/AOSLO studies reporting cone density at specific retinal eccentricities should be interpreted cautiously.

Consistent with previous reports, we observed a moderate inverse association between AL and magnification-corrected cone density. Because AL and SE are biologically related, potential collinearity between these variables should be considered when interpreting the adjusted estimates. However, when the analyses were repeated using uncorrected cone density, the association with AL was substantially weaker and no longer statistically significant. This pattern was observed in both the correlation analysis and the GEE models, including the adjusted and outlier-excluded analyses. The difference between the corrected and uncorrected results is important because AL is directly included in the magnification-correction procedure. Thus, part of the association observed with magnification-corrected cone density may reflect

mathematical coupling introduced by AL-based image scaling. In addition, because the magnification correction was based on AL alone, residual scaling error cannot be excluded. Therefore, this association should be considered exploratory and should not be interpreted as evidence of an independent biological relationship between AL and cone density.

In addition to AL, refractive status has been investigated as a potential factor associated with cone photoreceptor characteristics. Photoreceptor changes have also been implicated in the development of myopia, and alterations in the cone mosaic have been reported in myopic eyes[20]. Additionally, studies have demonstrated the effects of myopia on cone cell density. Liang et al.[7] and Dabir et al.[5] reported significant reductions in cone density and regularity in high myopia, whereas Zhou et al.[4] observed reduced cone regularity in axial myopia. In contrast, we found no significant association between SE and magnification-corrected cone density. This may be related to the relatively narrow refractive range of our study population, which consisted primarily of emmetropic individuals and those with low myopia. Therefore, the lack of an association with SE in our study should be interpreted in the context of this restricted refractive range.

In addition to the absence of significant dominance-related differences, we observed no systematic interocular differences in cone density or cone diameter. However, agreement differed between the two cone metrics, with moderate agreement for cone density (ICC = 0.679) and poor agreement for cone diameter (ICC = 0.359). Therefore, the absence of a statistically significant mean interocular difference should not be interpreted as evidence of strong interocular agreement or equivalence. Cava et al.[21] similarly reported no significant interocular differences in foveal cone density and mosaic regularity in healthy individuals and found little evidence of a sex-related difference in foveal cone density, although a small sex-related difference in cone diameter was observed. In our adjusted analyses, sex was not independently associated with either magnification-corrected cone density or cone diameter. Park et al.[18] also found that ocular dominance was not a significant determinant of cone density and observed no meaningful differences between dominant and nondominant eyes, while Zhang et al.[3] reported similar total foveal cone numbers between fellow eyes. The weaker interocular agreement observed for cone diameter may be related to image resolution, automated segmentation, or the device-specific definition of this metric. Overall, our findings indicate an absence of systematic interocular bias but also show measurable interocular variability, particularly for cone diameter.

Within-eye repeatability was good for both cone density and cone diameter after exclusion of measurements with automated segmentation failure. Bland–Altman analysis similarly indicated little systematic difference between repeated acquisitions. Repeatability deteriorated when the segmentation-failure measurements were retained, highlighting the potential influence of segmentation failure on individual measurements and the importance of careful review of automated outputs.

Cone diameter requires more cautious interpretation. Although no systematic interocular difference was observed, its interocular agreement was weaker than that of cone density. This may partly reflect image resolution, automated cone boundary detection, and the device-specific definition of this metric. In the present system, mean cone diameter is generated automatically by the proprietary cone recognition and analysis software without manual measurement or modification by the investigators. Therefore, cone diameter should be regarded as a device-specific quantitative metric rather than a direct anatomical measurement of individual cone photoreceptors. Further validation against established high-resolution imaging techniques or independently derived cone measurements is needed to determine its accuracy. The strong inverse association between cone density and cone diameter should also be interpreted cautiously, as an inverse relationship between cone size and the number of cones within a given retinal area is geometrically expected and may not represent an independent biological association.

Several studies have evaluated the effects of age on cone photoreceptor density and morphology. Song et al.[15] compared younger (22–35 years) and older (50–65 years) individuals using AOSLO and reported no significant effect of age on cone density. Jacob et al.[22] similarly found no age-related differences in cone mosaic metrics using AO imaging. In contrast, Park et al. [18] reported a negative correlation between cone density and age, while Tumahai et al.[6] demonstrated an age-related reduction in perifoveal cone density in a population ranging from 6 to 78 years of age. In the present study, age was not significantly associated with either magnification-corrected or uncorrected cone density. This finding may be related to the relatively narrow age range of our participants, which may have limited our ability to detect age-related differences.

This study is among the few clinical studies evaluating cone photoreceptor measurements obtained using an automated confocal cone analysis system in healthy human eyes. A strength of the study is the presentation of preliminary device-specific reference values obtained using this platform in healthy young adults. In addition, within-eye repeatability, interocular differences and agreement, ocular dominance, and biometric associations were evaluated, with appropriate statistical methods used to account for the

paired-eye structure of the data. The evaluation of both magnification-corrected and uncorrected cone density also allowed the potential influence of AL-based magnification correction on the observed associations to be examined. Overall, these findings provide an initial characterization of cone photoreceptor measurements obtained with this automated confocal imaging platform. Further studies comparing these measurements with established high-resolution imaging techniques are needed to determine their accuracy and clinical applicability.

Several limitations should be considered when interpreting our findings. First, the sample size was relatively modest, and the study included only healthy young adults with restricted ranges of refractive error and AL. Therefore, the reported measurements should be considered preliminary device-specific reference values for this population rather than normative data for the general population. Second, recruitment from healthy volunteers may further limit the generalizability of the findings. Third, the MicroClear CRO platform does not currently provide additional cone mosaic metrics such as spacing, regularity, or nearest-neighbor analyses. Although within-eye repeatability was evaluated, occasional measurements with automated segmentation failure were observed, highlighting the need for careful review of automated outputs. External validation against established AO imaging systems or independent manual cone counts was not performed; therefore, the absolute accuracy of the automated cone measurements remains unknown. Further studies using established high-resolution imaging techniques are needed to validate these measurements. Finally, AL was the only biometric parameter used for magnification correction and was itself incorporated into the correction procedure. This may introduce mathematical coupling and residual scaling error when examining the relationship between AL and corrected cone density. Although the analysis of uncorrected cone density helped assess this issue, associations based on magnification-corrected measurements should be interpreted cautiously.

In conclusion, this study provides preliminary device-specific reference values for cone photoreceptor measurements obtained using an automated confocal cone analysis system in healthy young adults, with good within-eye repeatability for both cone density and cone diameter after exclusion of measurements with automated segmentation failure. No systematic interocular differences were observed, although interocular agreement was moderate for cone density and poor for cone diameter. No association with ocular dominance was identified. The association between AL and cone density differed substantially between magnification-corrected and uncorrected measurements, indicating that this relationship is sensitive to the magnification-correction procedure and should be interpreted cautiously. Further studies in larger and more diverse populations, together with external validation against established high-resolution imaging methods, are needed to establish the accuracy and clinical utility of this platform.

Researcher Contribution Statement:
Concept and design: S.K., G.C., O.K.; Data collection and processing: O.K., G.C., S.K., B.B.O.; Analysis and interpretation of data: F.K., B.B.O., S.K.; Drafting of the manuscript: S.K., F.K.; Critical revision of the manuscript for important intellectual content: G.C., O.K., B.B.O., F.K., S.K.; Final approval of the version to be published: All authors; Accountability for all aspects of the work: All authors.

Conflict of Interest Statement:
The authors of the article have no conflict of interest declarations.

Ethics Committee Approval Information:
Approving Committee: Zeynep Kamil Maternity and Children's Diseases Training and Research Hospital
Approval Date: 08/27/2025
Decision No: 97

References

1. Behar-Cohen F, Gelize E, Jonet L, et al. [Anatomy of the retina]. Med Sci (Paris) 2020; 36: 594–599. 20200702. DOI: 10.1051/medsci/2020094.
2. Lamb TD. Why rods and cones? Eye (Lond) 2016; 30: 179–185. 20151113. DOI: 10.1038/eye.2015.236.
3. Zhang T, Godara P, Blanco ER, et al. Variability in Human Cone Topography Assessed by Adaptive Optics Scanning Laser Ophthalmoscopy. Am J Ophthalmol 2015; 160: 290–300 e291. 20150430. DOI: 10.1016/j.ajo.2015.04.034.
4. Zhou WD, Dong L, Shi HX, et al. Cone mosaic in eyes with varied axial length using adaptive optics scanning laser ophthalmoscopy. Photodiagnosis Photodyn Ther 2025; 52: 104517. 20250208. DOI: 10.1016/j.pdpdt.2025.104517.
5. Dabir S, Mangalesh S, Schouten JS, et al. Axial length and cone density as assessed with adaptive optics in myopia. Indian J Ophthalmol 2015; 63: 423–426. DOI: 10.4103/0301-4738.159876.
6. Tumahai P, Moureaux C, Meillat M, et al. High-resolution imaging of photoreceptors in healthy human eyes using an adaptive optics retinal camera. Eye (Lond) 2018; 32: 1723–1730. 20180711. DOI: 10.1038/s41433-018-0140-1.
7. Liang J, Fang D, Diao Y, et al. Photoreceptor cone loss is associated with decreased deep retinal vessel density and impaired retinal sensitivity in high myopia. Br J Ophthalmol 2025; 109: 1194–1200. 20250923. DOI: 10.1136/bjo-2024-326609.
8. Wang Y, Bensaid N, Tiruveedhula P, et al. Human foveal cone photoreceptor topography and its dependence on eye length. Elife 2019; 8 20190726. DOI: 10.7554/eLife.47148.
9. Reumueller A, Wassermann L, Salas M, et al. Three-dimensional composition of the photoreceptor cone layers in healthy eyes using adaptive-optics optical coherence tomography (AO-OCT). PLoS One 2021; 16: e0245293. 20210107. DOI: 10.1371/journal.pone.0245293.
10. Jackson K, Vergilio GK, Cooper RF, et al. A 2-Year Longitudinal Study of Normal Cone Photoreceptor Density. Invest Ophthalmol Vis Sci 2019; 60: 1420–1430. DOI: 10.1167/iovs.18-25904.
11. Cooper RF, Kalaparambath S, Aguirre GK, et al. Morphology of the normative human cone photoreceptor mosaic and a publicly available adaptive optics montage repository. Sci Rep

2024; 14: 23166. 20241005. DOI: 10.1038/s41598-024-74274-y.

12. Bennett AG, Rudnicka AR and Edgar DF. Improvements on Littmann's method of determining the size of retinal features by fundus photography. Graefes Arch Clin Exp Ophthalmol 1994; 232: 361–367. DOI: 10.1007/BF00175988.
13. Shen Y, Ye X, Zhou X, et al. In vivo assessment of cone loss and macular perfusion in children with myopia. Sci Rep 2024; 14: 26373. 20241102. DOI: 10.1038/s41598-024-78280-y.
14. Li KY, Tiruveedhula P and Roorda A. Intersubject variability of foveal cone photoreceptor density in relation to eye length. Invest Ophthalmol Vis Sci 2010; 51: 6858–6867. 20100804. DOI: 10.1167/iovs.10-5499.
15. Song H, Chui TY, Zhong Z, et al. Variation of cone photoreceptor packing density with retinal eccentricity and age. Invest Ophthalmol Vis Sci 2011; 52: 7376–7384. 20110921. DOI: 10.1167/iovs.11-7199.
16. Gocho K, Sarda V, Falah S, et al. Adaptive optics imaging of geographic atrophy. Invest Ophthalmol Vis Sci 2013; 54: 3673–3680. 20130501. DOI: 10.1167/iovs.12-10672.
17. Kitaguchi Y, Bessho K, Yamaguchi T, et al. In vivo measurements of cone photoreceptor spacing in myopic eyes from images obtained by an adaptive optics fundus camera. Jpn J Ophthalmol 2007; 51: 456–461. 20071221. DOI: 10.1007/s10384-007-0477-7.
18. Park SP, Chung JK, Greenstein V, et al. A study of factors affecting the human cone photoreceptor density measured by adaptive optics scanning laser ophthalmoscope. Exp Eye Res 2013; 108: 1–9. 20121228. DOI: 10.1016/j.exer.2012.12.011.
19. Legras R, Gaudric A and Woog K. Distribution of cone density, spacing and arrangement in adult healthy retinas with adaptive optics flood illumination. PLoS One 2018; 13: e0191141. 20180116. DOI: 10.1371/journal.pone.0191141.
20. Wang K, Han G and Hao R. Advances in the study of the influence of photoreceptors on the development of myopia. Exp Eye Res 2024; 245: 109976. 20240617. DOI: 10.1016/j.exer.2024.109976.
21. Cava JA, Allphin MT, Mastey RR, et al. Assessing Interocular Symmetry of the Foveal Cone Mosaic. Invest Ophthalmol Vis Sci 2020; 61: 23. DOI: 10.1167/iovs.61.14.23.
22. Jacob J, Paques M, Krivosic V, et al. Comparing Parafoveal Cone Photoreceptor Mosaic Metrics in Younger and Older Age Groups Using an Adaptive Optics Retinal Camera. Ophthalmic Surg Lasers Imaging Retina 2017; 48: 45–50. DOI: 10.3928/23258160-20161219-06.